Chromosoma (2012) 121:209–220
DOI 10.1007/s00412-011-0355-4

RESEARCH ARTICLE

The chromodomain-containing NH_2-terminus of Chromator interacts with histone H1 and is required for correct targeting to chromatin

Changfu Yao · Yun Ding · Weili Cai · Chao Wang · Jack Girton · Kristen M. Johansen · Jørgen Johansen

Received: 10 August 2011 / Revised: 22 November 2011 / Accepted: 9 December 2011 / Published online: 28 December 2011

Abstract The chromodomain protein, Chromator, can be divided into two main domains, a NH_2-terminal domain (NTD) containing the chromodomain (ChD) and a COOH-terminal domain (CTD) containing a nuclear localization signal. During interphase Chromator is localized to chromosomes; however, during cell division Chromator redistributes to form a macro molecular spindle matrix complex together with other nuclear proteins that contribute to microtubule spindle dynamics and proper chromosome segregation during mitosis. It has previously been demonstrated that the CTD is sufficient for targeting Chromator to the spindle matrix. In this study, we show that the NTD domain of Chromator is required for proper localization to chromatin during interphase and that chromosome morphology defects observed in Chromator hypomorphic mutant backgrounds can be largely rescued by expression of this domain. Furthermore, we show that the ChD domain can interact with histone H1 and that this interaction is necessary for correct chromatin targeting. Nonetheless, that localization to chromatin still occurs in the absence of the ChD indicates that Chromator possesses a second mechanism for chromatin association and we provide evidence that this association is mediated by other sequences residing in the NTD. Taken together these findings suggest that Chromator's chromatin functions are largely governed by the NH_2-terminal domain whereas functions related to mitosis are mediated mainly by COOH-terminal sequences.

Communicated by Sergio Pimpinelli

C. Yao · Y. Ding · W. Cai · C. Wang · J. Girton · K. M. Johansen · J. Johansen (✉)
Department of Biochemistry, Biophysics, and Molecular Biology, Iowa State University, 3156, Molecular Biology Building, Ames, IA 50011, USA
e-mail: jorgen@iastate.edu

Introduction

The chromodomain protein, Chromator, has multiple functions depending on the developmental context (Rath et al. 2006; Mendjan et al. 2006; Wasser et al. 2007; Ding et al. 2009). During interphase Chromator is localized to interband regions of *Drosophila* polytene chromosomes (Rath et al. 2004; Gortchakov et al. 2005) and has been demonstrated to interact with other chromosomal proteins such as the zinc-finger protein Z4 (Eggert et al. 2004; Gan et al. 2011) and the histone H3S10 kinase JIL-1 (Rath et al. 2006) and to contribute to the maintenance of polytene chromosome morphology (Rath et al. 2006). However, during cell division Chromator redistributes to form a macro molecular spindle matrix complex together with at least three other nuclear-derived proteins Skeletor, Megator, and EAST (Walker et al. 2000; Rath et al. 2004; Qi et al. 2004, 2005). It has recently been proposed that this structure may take the form of a hydrogel-like matrix with viscoelastic properties that contribute to microtubule spindle dynamics and proper chromosome segregation during mitosis (Johansen et al. 2011). Evidence that Chromator may participate in spindle matrix function has been provided by mutational analysis with two loss-of-function alleles, $Chro^{71}$ and $Chro^{612}$ (Ding et al. 2009). The analysis showed that neuroblasts from $Chro^{71}/Chro^{612}$ brain squash preparations have severe microtubule spindle and chromosome segregation defects that were associated with a developmental small brain phenotype. Furthermore, time-lapse analysis of mitosis in S2 cells depleted of Chromator by RNAi treatment suggested that the chromosome segregation defects were the results of incomplete alignment of chromosomes at the metaphase plate, possibly due to a defective spindle assembly checkpoint, as well as of frayed and unstable microtubule spindles during anaphase (Ding et al. 2009).

Chromator can be divided into two main domains, an NH_2-terminal domain (NTD) containing the chromodomain (ChD) and a COOH-terminal domain (CTD) containing a nuclear localization signal (Rath et al. 2004). The studies of Ding et al. (2009) showed that the CTD of Chromator was sufficient for localization to spindles and that expression of this domain alone could partially rescue mutant spindle defects. However, the function of the NTD and whether it plays a role in targeting Chromator to chromatin was not determined. Here we provide evidence that the NTD of Chromator is responsible for correct targeting to chromatin, that it interacts with histone H1, and that the chromodomain is required for these interactions.

Materials and methods

Chromator transgenic constructs

A Chromator full-length (1-926) construct (FL) was inserted into the pUASP vector (Brand and Perrimon 1993) with an N-terminal TAP tag (3xHA, 3xFlag) and a C-terminal GFP tag using standard methods (Sambrook and Russell 2001). The Chromator NTD construct (1–346) and the CTD construct (329–926) in the pUASP vector have been previously described in Ding et al. (2009). The CTD of Chromator contains the endogenous nuclear localization signal (NLS) (Rath et al. 2004). The ChD construct (219–277) was cloned into the pUAST vector and included three in-frame NLS sequences cut from the pECFP-Nuc vector (Clontech) followed by in-frame V5- and GFP tags. The NTD−ΔChD construct (1–219) was cloned into the pUAST vector and contained three in-frame NLS sequences in addition to an in-frame V5 tag. The fidelity of all constructs was verified by sequencing at the Iowa State University DNA Facility.

Drosophila melanogaster stocks

Fly stocks were maintained according to standard protocols (Roberts 1998). Canton S was used for wild-type preparations. The *Chromator* mutant alleles $Chro^{71}$ and $Chro^{612}$ as well as the transheterozygous $Chro^{71}/Chro^{612}$ allelic combination have been previously described in Rath et al. (2006) and in Ding et al. (2009). Chromator construct pUAST or pUASP transgenic lines were generated by standard P-element transformation (BestGene, Inc.), and expression of the transgenes was driven using the *hsp70-GAL4* (*P{w[+mC] = GAL4-hsp70.PB}*) driver or the *Sgs3-GAL4*(*P{w[+mC] = Sgs3-GAL4.PD}TP1*) driver (obtained from the Bloomington Stock Center; stocks 5704 and 6870, respectively) introduced by standard genetic crosses. For heat shock experiments, larvae were subjected to 30 min of heat shock treatment at 37°C as described previously (Nowak et al. 2003). Balancer chromosomes and markers are described in Lindsley and Zimm (1992).

Immunohistochemistry

Standard polytene chromosome squash preparations were performed as in Cai et al. (2010) using either 1 or 5 min fixation protocols and labeled with antibody as described in Jin et al. (1999) and in Wang et al. (2001). Primary antibodies used included chicken anti-GFP (Aves Labs), anti-V5 antibody (Invitrogen), anti-H1 antibody (Active Motif), as well as anti-Chromator mAbs 6H11 and 12H9 (Rath et al. 2004). DNA was visualized by staining with Hoechst 33258 (Molecular Probes) in PBS. The appropriate species- and isotype-specific Texas Red-, TRITC-, and fluorescein isothiocyanate-conjugated secondary antibodies (Cappel/ICN, Southern Biotech) were used (1:200 dilution) to visualize primary antibody labeling. The final preparations were mounted in 90% glycerol containing 0.5% *n*-propyl gallate. The preparations were examined using epifluorescence optics on a Zeiss Axioskop microscope, and images were captured and digitized using a Spot CCD camera. Images were imported into Photoshop where they were pseudocolored, image processed, and merged. In some images, nonlinear adjustments were made to the channel with Hoechst labeling for optimal visualization of chromosomes.

For live imaging of polytene chromosomes, third instar larvae salivary glands were dissected and mounted in physiological saline (110 mM NaCl, 4 mM KCl, 2 mM $CaCl_2$, 10 mM glucose, 10 mM HEPES, pH 7.4) as in Deng et al. (2005). In some cases, 25–50% glycerol was added to the physiological saline in order to prevent drift of the preparations. The larvae were from transgenic animals carrying the GFP-tagged FL, NTD, ChD, or CTD expressed in a $Chro^{71}/Chro^{612}$ mutant background. Confocal images were obtained using a Leica confocal TCS SP5 microscope system.

Immunoblot analysis

Protein extracts were prepared from whole third instar larvae or in some experiments from dissected salivary glands homogenized in a buffer containing: 20 mM Tris–HCl pH 8.0, 150 mM NaCl, 10 mM EDTA, 1 mM EGTA, 0.2% Triton X-100, 0.2% NP-40, 2 mM Na_3VO_4, 1 mM PMSF, and 1.5 μg/ml aprotinin. Proteins were separated by SDS-PAGE according to standard procedures (Sambrook and Russell 2001). Electroblot transfer was performed as in Towbin et al. (1979) with transfer buffer containing 20% methanol and in most cases including 0.04% SDS. For these experiments, we used the Bio-Rad Mini PROTEAN III system, electroblotting to 0.2-μm nitrocellulose membrane, and using anti-mouse or anti-rabbit HRP-conjugated secondary antibody (Bio-Rad) (1:3,000) for visualization of primary antibody. In some

experiments labeling with anti-tubulin antibody (Sigma-Aldrich) was used as a loading control. Antibody labeling was visualized using chemiluminescent detection methods (SuperSignal West Pico Chemiluminescent Substrate, Pierce). The immunoblots were digitized using a flatbed scanner (Epson Expression 1680).

Overlay experiments

For overlay experiments GST-tagged versions of the full-length or truncated Chromator constructs, GST–FL (1–926), GST–NTD (1–346), GST–ChD (219–277), GST–NTD–ΔChD (1–218), and GST–CTD (329–926) were generated using standard methods (Sambrook and Russell 2001). The respective GST fusion proteins were expressed in BL21 cells and purified over a glutathione agarose column (Sigma-Aldrich) according to the pGEX manufacturer's instructions (Amersham Biosciences). In addition, a full-length *Drosophila* histone H1 fusion protein with a maltose binding protein-tag (MBP) was generated in the pMAL-c2x vector (NEB), expressed in BL21 cells, and purified over an amylose resin column (NEB) according to the pMAL manufacturer's instructions (NEB). For the overlay interaction assays, either individually purified bovine histones (Roche Applied Science), *Drosophila* histone H1 (MBP-H1), or MBP only was fractionated by SDS-PAGE and electroblotted to nitrocellulose. The blots were subsequently incubated with 2 μg of either GST–FL, GST–NTD, GST–ChD, GST–NTD–ΔChD, or GST–CTD fusion protein overnight at 4°C in PBS with 0.5% Tween 20 and 5% nonfat milk on a rotating wheel. The blots were washed four times for 10 min each in 2× PBS with 0.1% Tween 20 (PBS-T), and binding was detected by anti-GST mAb 8C7 (Rath et al. 2004). In addition, the overlay proteins were separated by SDS-PAGE, electroblotted to nitrocellulose, and visualized by Ponceu S or Coomassie Blue staining (Sambrook and Russell 2001). The cDNA sequence for all fusion proteins was verified by sequencing.

Pull-down experiments

For in vitro pull-down assays with the GST-tagged Chromator fusion proteins, a His-tagged (6×) *Drosophila* histone H1 fusion protein (His–H1) as well as a His-tagged control fusion protein (His–JIL-1) containing the NH_2-terminal of JIL-1 (1–260) (Jin et al. 1999) were generated in the pET-28a vector (Novagen). The His–H1, His–JIL-1, and Chromator–GST fusion proteins were expressed in BL-21 cells. For GST pull-down assays, approximately 3 μg of GST–Chromator fusion proteins or GST protein alone were coupled to glutathione agarose beads (Sigma) and incubated with 3 μg His–H1 protein in immunoprecipitation (ip) buffer (20 mM Tris–HCl pH 8.0, 10 mM EDTA, 1 mM EGTA, 150 mM NaCl, 0.1% Triton X-100, 0.1% Nonidet P-40, 1 mM phenylmethylsulfonyl fluoride, and 1.5 μg aprotinin) overnight at 4°C. The protein complex-coupled beads were washed five times for 10 min each with 1 ml of 2× PBS-T and analyzed by SDS-PAGE and immunoblotting using anti-H1 antibody (Active Motif). For pull-down assays with His-tagged proteins, 3 μg of His–H1 or His–JIL-1 was bound to Ni-NTA beads (QIAGEN) and incubated with 3 μg of Chromator–GST fusion protein in 500 μl of immunoprecipitation buffer. The protein complex-coupled beads were washed five times for 10 min each with 1 ml 2× PBS-T and analyzed by SDS-PAGE and immunoblotting using the GST mAb 8C7 (Rath et al. 2004).

For native protein pull-down assays, *Drosophila* S2 cell nuclear extract was prepared as described in Kusch et al. (2003). For GST pull-down assays GST–ChD (2 μg), GST protein alone (2 μg) or GST–CTD (6 μg) at molar ratios was coupled with glutathione agarose beads and incubated with 500 μl of S2 cell nuclear extract at 4°C overnight. The beads were washed five times for 10 min each in 1 ml of ip buffer, and proteins retained on the glutathione agarose beads were analyzed by SDS-PAGE and immunoblotting using anti-H1 antibody. For pull-down assays with His-tagged proteins, 3 μg of His–H1 or 3.5 μg of His–JIL-1 was bound to Ni-NTA beads (QIAGEN) and incubated with 500 μl of S2 cell nuclear extract at 4°C overnight. The protein complex-coupled beads were washed five times for 10 min each with 1 ml ip buffer and proteins retained on the beads analyzed by SDS-PAGE and immunoblotting using the Chromator mAb 6H11 (Rath et al. 2004).

Co-immunoprecipitation experiments

For co-immunoprecipitation experiments, the GFP-tagged FL, NTD, ChD, and CTD transgenes were each expressed in adult flies using the *hsp70-GAL4* driver. Protein lysate was prepared for each genotype as well as wild-type controls by homogenizing 50 adult flies in 2 ml of ip buffer and collecting the supernatant after centrifugation at 4,000 rpm for 10 min. Transgene protein expression in the lysates was verified by SDS-PAGE and immunoblot analysis using a rabbit anti-GFP mAb (Cell Signaling). Immunobeads were prepared by coupling 5 μl of chicken anti-GFP antibody (Aves Lab) to 30 μl of anti-IgY immobilized agarose beads (Pierce) for 2.5 h at 4°C on a rotating wheel in 300 μl ip buffer. The antibody-coupled beads were subsequently incubated in 500 μl of fly lysate overnight at 4°C. The protein complex-coupled beads were washed five times for 10 min each with 1 ml ip buffer, and proteins retained on the beads analyzed by SDS-PAGE and immunoblotting using anti-H1 antibody.

Modeling

The structure of the chromodomain of Chromator was modeled with the I-TASSER protein prediction server (Zhang 2007;

Roy et al. 2010) and compared to the crystal structure of *Drosophila* HP1a's chromodomain (PDB ID: 1Q3L). I-TASSER generates models of proteins by excising continuous fragments from Local Meta-Threading-Server multiple-threading alignments and then reassembling them using replica-exchange Monte Carlo simulations (Zhang 2008). The comparison and visualization between the model of Chromator's chromodomain and HP1a's chromodomain was processed and rendered by PyMOL.

Results

The NTD is required for correct targeting of Chromator to chromatin

In order to undertake a structure/function analysis of the Chromator protein, we expressed deletion constructs transgenically in flies heterozygous for the two hypomorphic loss-of-function *Chromator* alleles, $Chro^{71}$ and $Chro^{612}$ as in Rath et al. (2006) and in Ding et al. (2009). The $Chro^{71}$ allele is comprised of a G to A nucleotide change at nucleotide position 402 of the *Chromator* transcribed sequence that introduces a premature stop codon resulting in a truncated 71 amino acid protein (Rath et al. 2006). The truncated NH_2-terminal fragment does not contain the chromodomain and $Chro^{71}$ is likely to act as a null allele. $Chro^{71}$ is homozygous embryonic lethal with no first instar larval escapers. The $Chro^{612}$ allele consists of a C to T nucleotide change at nucleotide position 2024 that introduces a premature stop codon resulting in a truncated 612 amino acid protein that retains the chromodomain (Rath et al. 2006) but is missing parts of the COOH-terminal domain important for spindle localization (Rath et al. 2004) and for interactions with Skeletor (Rath et al. 2004) and EAST (Wasser et al. 2007). $Chro^{71}/Chro^{612}$ transheterozygotes survive to third instar larval stages although no larvae have been observed to pupate. Figure 1a, b shows a comparison of polytene squashes from wild-type and $Chro^{71}/Chro^{612}$ larvae labeled with Hoechst and the Chromator mAbs 6H11 and 12H9, respectively. mAb 6H11 recognizes an epitope specific to the CTD whereas mAb 12H9 recognizes an epitope specific to the NTD (Rath et al. 2004, 2006; Ding et al. 2009). Whereas wild-type polytene chromosomes show extended arms with a regular pattern of Hoechst stained bands (Fig. 1a, b); this pattern is severely perturbed in $Chro^{71}/Chro^{612}$ mutant larvae (Fig. 1a, b). In the latter preparations, band/interband regions were disrupted and the chromosome arms were coiled and condensed (Fig. 1a, b) (Rath et al. 2006). The immunoblot of protein extracts from wild-type and $Chro^{71}/Chro^{612}$ third instar larvae in Fig. 1c demonstrates that no detectable full-length Chromator protein was present in the mutant larvae. However, weak labeling of $Chro^{71}/Chro^{612}$ mutant polytene chromosomes could occasionally be detected with mAb 12H9 (Fig. 1b).

In order to explore the role of the different Chromator domains in chromosome targeting, we expressed five GFP- and/or V5-tagged Chromator UAS P-element insertion constructs transgenically in $Chro^{71}/Chro^{612}$ mutant animals: a full-length construct (FL), a construct without the COOH-terminal domain (NTD), a construct containing only the COOH-terminal region (CTD), a construct containing the NTD but without the chromodomain (NTD−ΔChD), and a construct with the ChD only (Fig. 2). In these studies a *hsp70-GAL4* or a *SgG3-GAL4* driver line was used. As previously reported (Ding et al. 2009), expression of a full-length Chromator construct in the $Chro^{71}/Chro^{612}$ mutant background rescued all aspects of the mutant phenotype studied including lethality, microtubule spindle morphology, brain and salivary gland size, and polytene chromosome morphology.

As a first approach to determine which domain of Chromator is responsible for localization to chromatin, we expressed GFP-tagged FL, NTD, ChD, and CTD constructs in a $Chro^{71}/Chro^{612}$ mutant background and obtained confocal images from live polytene nuclei. As illustrated in Fig. 3, the FL and NTD localized to the polytene chromosomes in a banded pattern, whereas the localization of the ChD, while clearly present on the chromosomes, was more diffuse. In contrast, the CTD was found exclusively in the intranuclear space surrounding the chromosomes. These findings suggested that Chromator's affinity for chromatin is mediated by sequences in the NTD. To further explore this possibility at higher resolution, we expressed the ChD and the NTD−ΔChD in addition to the FL, NTD, and CTD in the $Chro^{71}/Chro^{612}$ mutant background and prepared polytene chromosome squash preparations labeled with Chromator, GFP, or V5 antibody to identify the constructs as well as with Hoechst. As illustrated in Fig. 4 expression of the FL rescued, all aspects of the mutant polytene chromosome morphology and the localization of the FL to interband regions were indistinguishable from that of native Chromator in wild-type preparations (Fig. 1) as also previously reported for a full-length Chromator construct under native promoter control (Ding et al. 2009). Interestingly, the NTD construct also substantially rescued polytene chromosome morphology although rescue was not complete with some remaining coiled regions of the chromosome arms (Fig. 4). It should be noted that the NTD unlike the FL did not rescue any aspects of the reduced size of brains, imaginal disks, or salivary glands. However, localization of the NTD to a majority of interband polytene chromosome regions was clearly discernable. In contrast, while both the ChD and the NTD−ΔChD localized to chromatin, no distinct banding pattern was apparent and there was no or very little improvement in the mutant polytene chromosome morphology (Fig. 4). For comparison, the CTD showed little or no chromatin binding affinity and there was no rescue of the mutant polytene chromosome morphology (Fig. 4). These findings confirm the results from

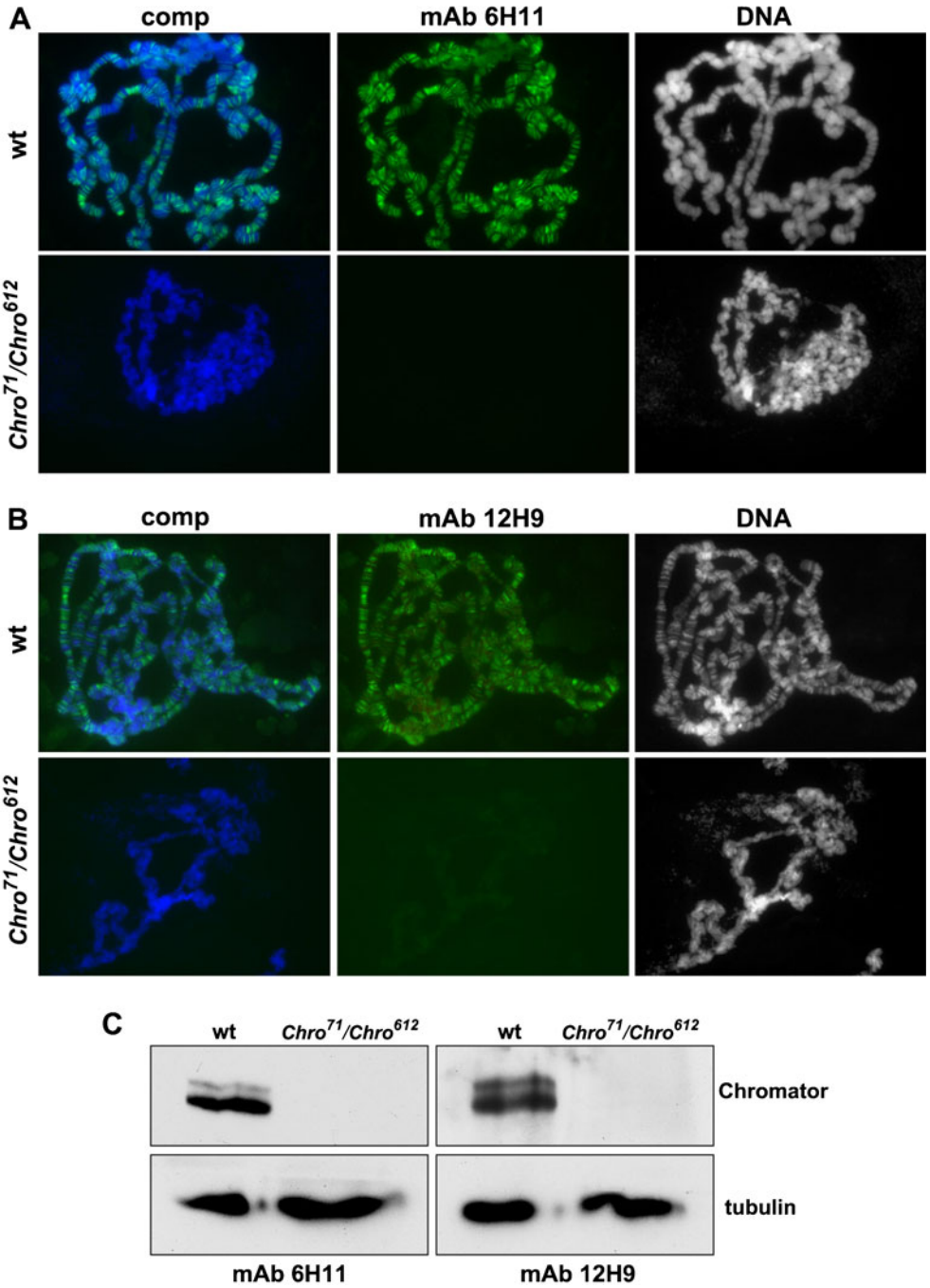

Fig. 1 Chromator expression in the hypomorphic $Chro^{71}/Chro^{612}$ mutant background. **a** Double labelings with the COOH-terminal Chromator mAb 6H11 (*green*) and Hoechst (*blue/gray*) of polytene squashes from wild-type (*upper panel*) and $Chro^{71}/Chro^{612}$ (*lower panel*) third instar larvae. The composite image (*comp*) is shown to the *left*. The mAb 6H11 epitope is not present in either of the truncated $Chro^{71}$ or $Chro^{612}$ proteins. **b** Double labeling with the NH_2-terminal Chromator mAb 12H9 (*green*) and Hoechst (*blue/gray*) of polytene squashes from a $Chro^{71}/Chro^{612}$ third instar larvae. The composite image (*comp*) is shown to the *left*. **c** Immunoblot analysis of Chromator protein expression in $Chro^{71}/Chro^{612}$ mutant third instar larvae as compared to wild-type larvae. The immunoblots were labeled with the COOH-terminal Chromator mAb 6H11 (*left panel*), with the NH_2-terminal Chromator mAb 12H9 (*right panel*), and with anti-tubulin antibody as a loading control. Full-length Chromator is detected by both mAb 6H11 and 12H9 in wild-type larvae; however, no full-length Chromator is detectable in the mutant larvae

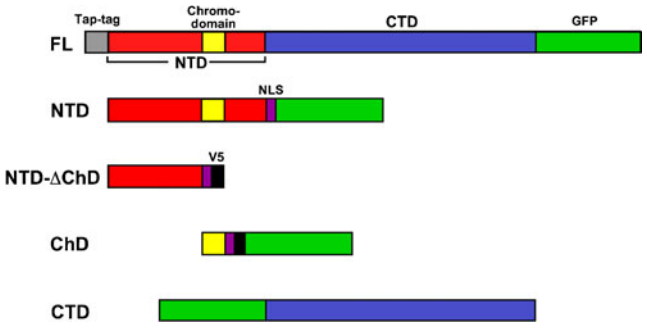

Fig. 2 Diagrams of the transgenic Chromator constructs analyzed

the imaging of live salivary gland nuclei that the NTD is largely responsible for correct targeting of Chromator to chromatin and further indicate that sequences from both the ChD and the NTD−ΔChD contribute to this localization.

The chromodomain of Chromator interacts with histone H1

The above polytene chromosome localization studies of the various Chromator domains indicated that both the ChD and the NTD−ΔChD may have the ability to bind to chromatin. Major constituents of chromatin include the linker histone

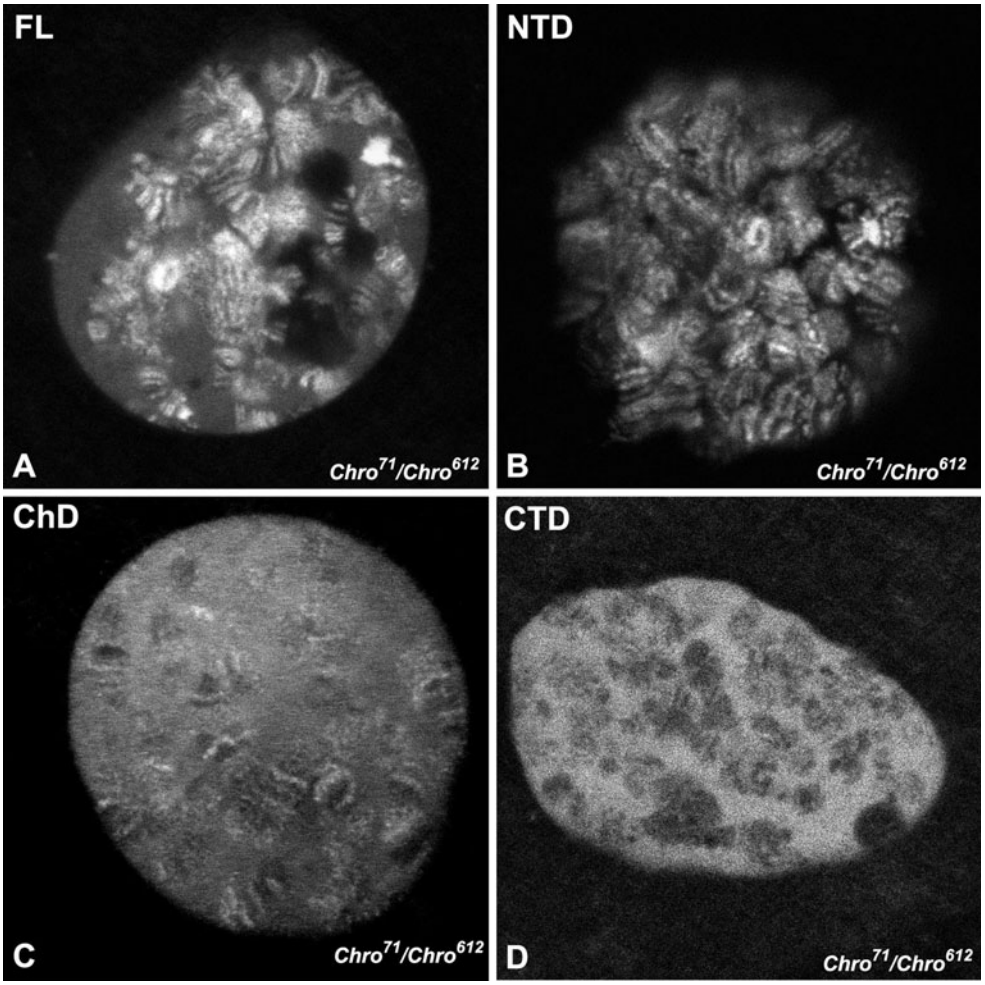

Fig. 3 Localization of transgenic Chromator GFP-tagged constructs in live salivary gland nuclei in a $Chro^{71}/Chro^{612}$ mutant background. The *FL* (**a**) and *NTD* (**b**) localizes to banded regions of the polytene chromosomes whereas the *ChD* (**c**), while present on the chromosomes, had a more diffuse localization. In contrast, the *CTD* was exclusively found in the intranuclear space surrounding the chromosomes (**d**). The images are from confocal sections

H1 and the histones H2A, H2B, H3, and H4 that together with DNA form nucleosomes (reviewed in Khorasanizadeh 2004). We therefore used overlay assays to test for interactions between these chromatin components and the various Chromator domains. For the screening we used GST-tagged versions of the Chromator constructs diagrammed in Fig. 2. In the overlay assays, purified bovine histones were fractionated by SDS-PAGE, transferred to nitrocellulose membrane, and incubated with glutathione agarose bead-purified GST–FL, GST–NTD, GST–ChD, GST–NTD−ΔChD, and GST–CTD, respectively. Protein interactions were detected with a mAb to GST. As illustrated in Fig. 5a–f, we found that the FL, NTD, and ChD, but not the NTD−ΔChD or the CTD, could specifically interact with bovine histone H1 in these assays. Taken together these results indicate that the chromodomain of Chromator can interact with bovine histone H1. However, histone H1 is the least phylogenetically conserved histone and to verify the interaction we made a MBP-tagged *Drosophila* histone H1 construct. As illustrated in Fig. 5g, h, overlay assays of the MBP-H1 construct performed as described above demonstrated that the Chromator chromodomain can interact with *Drosophila* histone H1. It should be noted that the very weak interaction of NTD−ΔChD with bovine H1 in Fig. 5e was not present with native *Drosophila* H1 (Fig. 5g) and was therefore likely to be nonspecific.

To further confirm the physical interaction of Chromator's chromodomain with histone H1, we performed in vitro pull-down experiments using a His-tagged histone H1 (His-H1) construct together with ChD–GST. Whereas CTD–GST or GST alone was not able to pull down His-H1, ChD-GST pulled down a band corresponding to the size of His-H1 (Fig. 6a). In the converse experiment, His-H1 was able to pull down ChD–GST using Ni-NTA-beads whereas a His-tagged construct of the NH_2-terminal domain of JIL-1 (Jin et al. 1999) or beads alone were not (Fig. 6b). These results support the existence of a direct physical interaction between Chromator's chromodomain and histone H1.

In order to explore whether the physical interaction of Chromator with histone H1 was physiological, we performed pull-down experiments with the His-H1 and ChD–GST constructs using S2 cell nuclear lysate (Fig. 6c, d).

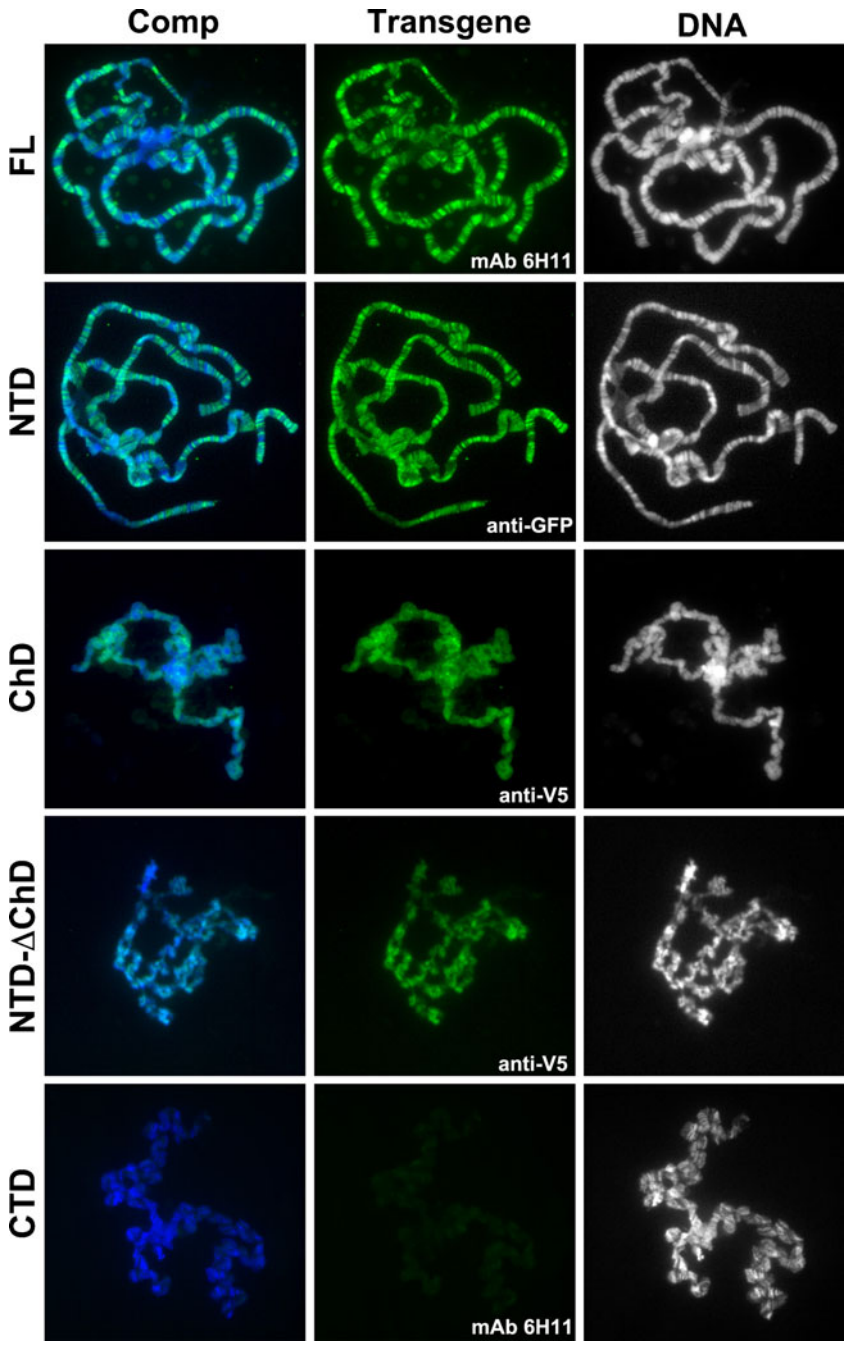

Fig. 4 Expression of Chromator deletion constructs transgenically in a $Chro^{71}/Chro^{612}$ mutant background. Polytene chromosome squash preparations from $Chro^{71}/Chro^{612}$ third instar larval salivary glands expressing the *FL*, *NTD*, *ChD*, *NTD−ΔChD*, and *CTD*, respectively. Transgene localization (*green*) was identified using either mAb 6H11 or anti-V5 or anti-GFP antibodies. DNA (*blue/gray*) was labeled by Hoechst

Whereas CTD–GST or GST alone was not able to pull down histone H1, ChD–GST pulled down a band corresponding to the size of histone H1 in the nuclear lysate as detected by anti-H1 antibody (Fig. 6c). In the converse experiment using Ni-NTA-beads, His-H1 was able to pull down a band corresponding to the size of Chromator in the nuclear lysate as detected with Chromator mAb 6H11 (Fig. 6d). In control lanes with a His-tagged construct of the NH_2-terminal domain of JIL-1 (Jin et al. 1999) or beads alone, no bands were detected (Fig. 6d). These results support the existence of a physical interaction between Chromator and histone H1.

To further confirm the physiological interaction, we performed ip experiments from flies expressing each of the four GFP-tagged transgenes FL, NTD, CTD, and ChD using GFP antibody. Protein lysate from 50 adult flies was prepared for each genotype as well as wild-type controls. Transgene protein expression in the lysates was verified by SDS-PAGE and immunoblot analysis using a rabbit anti-GFP mAb (Fig. 7a). The ChD and CTD were robustly expressed at comparable levels whereas the relative levels of FL and NTD were lower. In the ip experiments with anti-GFP antibody from these lysates, we found that a 38-kDa

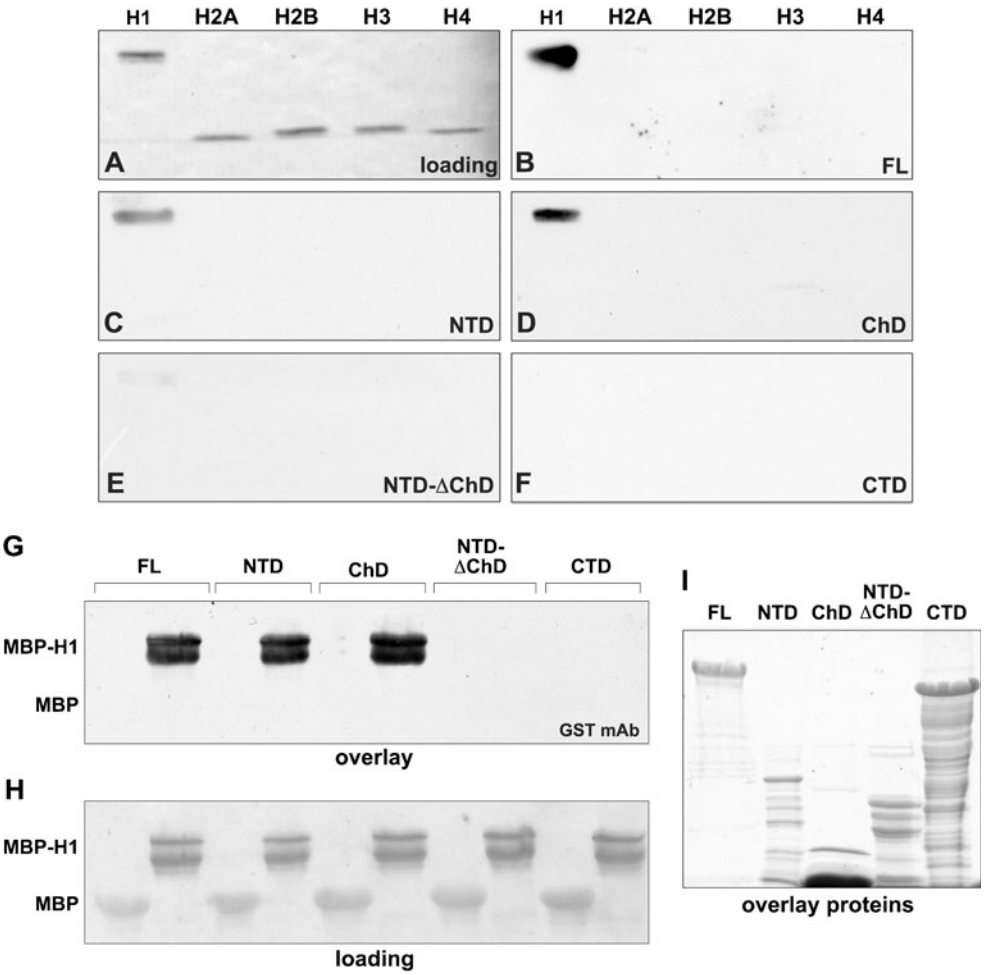

Fig. 5 The chromodomain of Chromator interacts with histone H1. **a**–**f** In overlay experiments, purified bovine histones were fractionated by SDS-PAGE, immunoblotted, incubated with Chromator GST–FL, GST–NTD, GST–ChD, GST–NTD−ΔChD, or GST–CTD fusion protein, and interactions detected with an anti-GST mAb (**b**–**f**). A representative Ponceau S labeling of the fractionated histone proteins is shown in (**a**). **g** In overlay experiments, a *Drosophila* histone H1 MBP-tagged fusion construct or MBP only was fractionated by SDS-PAGE, immunoblotted, incubated with Chromator GST–FL, GST–NTD, GST–ChD , GST–NTD−ΔChD, or GST–CTD fusion protein, and interactions detected with an anti-GST mAb. **h** Ponceau S labeling of the fractionated MBP–H1 and MBP proteins used for the overlay assay in (**g**). **i** A representative immunoblot of the GST fusion proteins used for the overlay experiments in (**b**–**g**) detected with Coomassie Blue

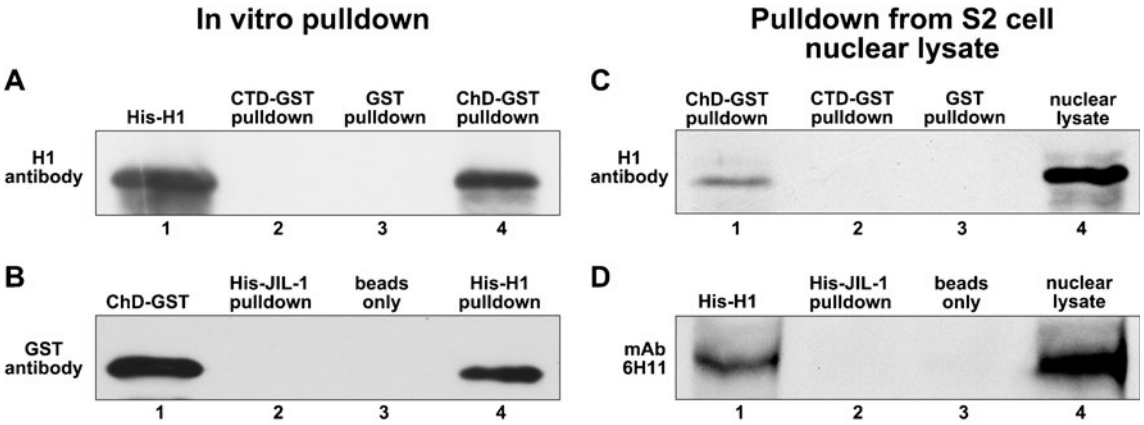

Fig. 6 Pull-down assays with Chromator's chromodomain and histone H1. **a** A ChD–GST construct pulled down His-tagged *Drosophila* histone H1 (*His-H1*) as detected by anti-H1 antibody (*lane 4*). A CTD–GST as well as a GST only control pulldown was negative (*lanes 2 and 3*, respectively). Lane 1 shows the His-H1 fusion protein. **b** A *Drosophila* His-H1 construct pulls down ChD–GST as detected by anti-GST antibody (*lane 4*). A control pulldown with a His-tagged construct of the NH_2-terminal domain of the JIL-1 kinase (His–JIL-1) or with beads only was negative (*lanes 2 and 3*, respectively). Lane 1 shows the ChD–GST fusion protein. **c** A ChD–GST construct pulled down a band corresponding to the size of histone H1 from S2 cell nuclear lysate as detected by anti-H1 antibody (*lane 1*). A CTD–GST as well as a GST only control pulldown was negative (*lanes 2 and 3*, respectively). Lane 4 shows the band in the nuclear lysate detected by H1 antibody. **d** A *Drosophila* His-H1 construct pulls down Chromator from S2 cell nuclear lysate as detected by the Chromator mAb 6H11 (*lane 1*). A control pulldown with a His-tagged construct with His–JIL-1 or with beads only was negative (*lanes 2 and 3*, respectively). Lane 4 shows the band in the nuclear lysate detected by mAb 6H11 antibody

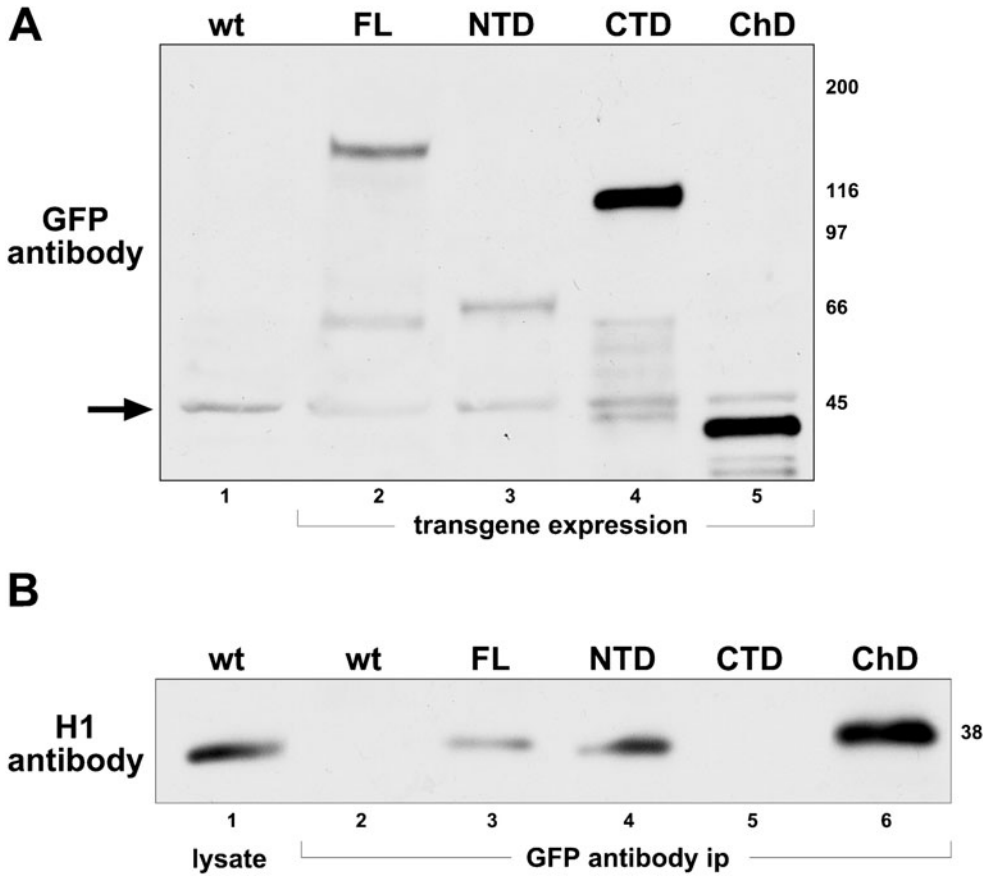

Fig. 7 Expression and co-immunoprecipitation analysis of protein lysates of flies expressing each of the four GFP-tagged transgenes FL, NTD, CTD, and ChD using anti-GFP antibody. **a** Protein lysate from wild-type (*wt*) flies and flies expressing the *FL*, *NTD*, *CTD*, or *ChD* transgenes analyzed by SDS-PAGE and immunoblotted using a rabbit anti-GFP mAb. The *arrow* indicates a background band also detected by the anti-GFP-antibody in wild-type fly lysate (*lane 1*). This band served as a loading control. The relative migration of molecular size markers is indicated to the right in kilodalton. **b** Anti-GFP-antibody ips from lysates of wild-type (*wt*) flies and of flies expressing the *FL*, *NTD*, *CTD*, or *ChD* transgenes analyzed by SDS-PAGE (4–15% gradient gel) and immunoblotted using H1 antibody (*lanes 2–6*). A 38-kDa protein band detected by anti-H1 antibody also present in lysate of wild-type flies (*lane 1*) was co-immunoprecipitated from lysate of flies expressing the FL, NTD, and ChD, but not from lysate of flies expressing the CTD (*lanes 3–6*). This 38-kDa band was not present in anti-GFP antibody ips from lysates of wild-type flies without transgene expression (*lane 2*)

protein band detected by H1 antibody also present in lysate of wild-type flies (Fig. 7b, lane 1) was immunoprecipitated from lysate of flies expressing the FL, NTD, and ChD, but not from lysate of flies expressing the CTD (Fig. 7b, lane 3–6). Furthermore, this 38-kDa band was not present in anti-GFP antibody ips from lysates of wild-type flies without transgene expression (Fig. 7b, lane 2). It should be noted that *Drosophila* histone H1 migrates anomalously on SDS gels with a shift of about 10 kDa (Siriaco et al. 2009).

Polytene chromosome immunolocalization of Chromator and H1

To determine the relative distribution of H1 and Chromator, we double labeled polytene squash preparations with Chromator mAb 6H11 and H1 antibody. As illustrated in Fig. 8a, histone H1 is predominantly present at band regions whereas Chromator is localized to interbands. However, histone H1 is also present at a lower density in the euchromatic interband regions (Hill et al. 1989). The interaction between H1 and Chromator is therefore likely to occur with the fraction of H1 present in interband chromatin or at the interface between interband and band regions. As illustrated in Fig. 8b, c, neither the ability to localize to chromatin nor the amount of H1 was affected in the $Chro^{71}/Chro^{612}$ mutant background as compared to wild type.

Modeling of the Chromator chromodomain

The chromodomain as well as the chromo-related domains constitute an evolutionary conserved module of about 50 amino acids that are widespread among eukaryotes (Paro and Hogness 1991; Gortchakov et al. 2005) and that perform a wide range of diverse functions (Brehm et al. 2004). The chromodomain in *Drosophila* most closely related to that of Chromator in structural database searches was that of

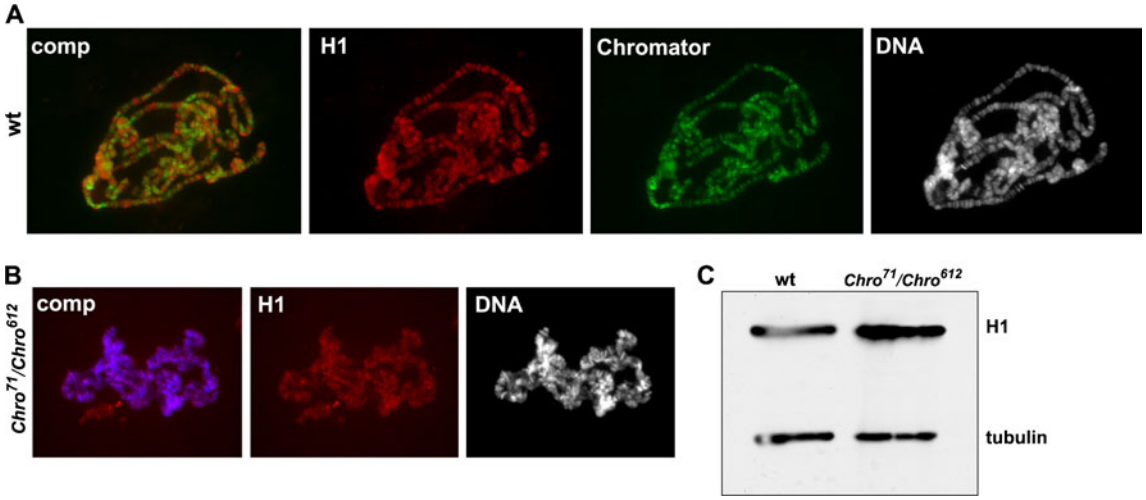

Fig. 8 H1 and Chromator chromosome localization. **a** Triple labeling with anti-H1 antibody (*red*), Chromator mAb 6H11 (*green*), and Hoechst (*blue/gray*) of a polytene squash from a wild-type third instar larvae. The composite image of H1 and Chromator labeling (*comp*) is shown to the *left*. **b** Double labeling with anti-H1 antibody (*red*) and Hoechst (*blue/gray*) of a polytene squash from a $Chro^{71}/Chro^{612}$ third instar larvae. The composite image (*comp*) is shown to the *left*. **c** Immunoblot analysis of H1 protein expression in $Chro^{71}/Chro^{612}$ mutant third instar larvae as compared to wild-type larvae. The immunoblots were labeled with anti-H1 antibody and with anti-tubulin antibody as a loading control

HP1a. HP1a is essential for the assembly of heterochromatin and its chromodomain is responsible for its binding to methylated histone H3 (Jacobs and Khorasanizadeh 2002). In order to compare the structure of Chromator's chromodomain with that of HP1a, we modeled it using the I-TASSER structure prediction program (Roy et al. 2010). As illustrated in Fig. 9, the spatial structure of the two chromodomains are very similar; however, two out of the three aromatic amino acids essential for binding to methylated histone H3 (Nielsen et al. 2001; Fischle et al. 2003) in the chromodomain of HP1a are not conserved and have been substituted with an arginine and aspartate residue, respectively (Gortchakov et al. 2005). In addition, the chromodomain of Chromator has an α-helical stretch before the main α-helix instead of a β-strand (Fig. 9). Thus, these changes may contribute to the chromodomain of Chromator's affinity for histone H1 instead of for methylated histone H3.

Discussion

In this study we show that the NTD domain of Chromator is required for proper localization to chromatin and that chromosome morphology defects observed in *Chromator* mutant backgrounds can be largely rescued by expression of this domain. We furthermore provide evidence that the ChD domain can interact with histone H1 suggesting that this interaction is necessary for the correct chromatin targeting. Nonetheless, that localization to chromatin still occurs in the absence of the ChD indicates that Chromator possesses a

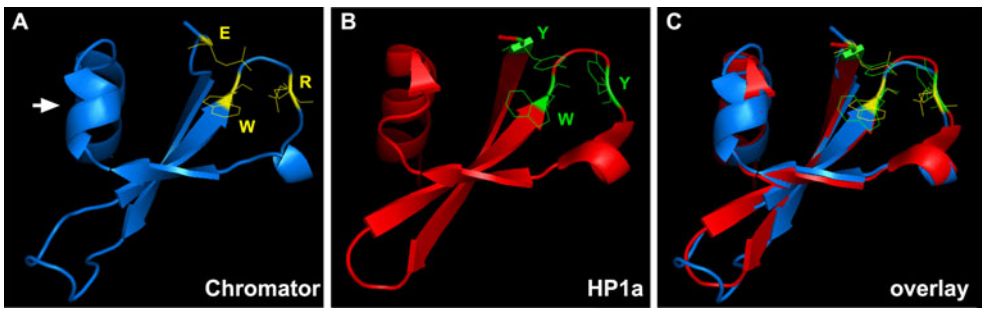

Fig. 9 Comparison of the structure of Chromator's chromodomain with that of HP1a. **a** Model of Chromator's chromodomain using the I-TASSER structure prediction platform (Roy et al. 2010). **b** The crystal structure of *Drosophila* HP1a's chromodomain (PDB ID: 1Q3L). **c** Overlay of the predicted structure of Chromator's chromodomain with that of HP1a. The three aromatic amino acids essential for binding to methylated histone H3 in the chromodomain of HP1a and the corresponding amino acids in Chromator's chromodomain are *highlighted*. The *arrow* in **a** indicates an α-helical stretch before the main α-helix instead of a β-strand in the chromodomain of Chromator. The structures were rendered in PyMOL

second mechanism for chromatin association and we provide evidence that this association is mediated by other sequences residing in the NTD. Such an association could in principle be mediated by other molecular interaction partners of Chromator that also localize to chromatin such as JIL-1 or Z4. However, studies in S2 cells with RNAi mediated Chromator depletion and in *JIL-1*^{z2} homozygous null mutant backgrounds demonstrated that neither protein was dependent on the other for its chromatin localization (Rath et al. 2006). The interaction of Chromator with Z4 was identified in co-immunoprecipitation experiments and the two proteins colocalize extensively at interband polytene regions (Eggert et al. 2004) Recently, Gan et al. (2011) provided evidence that Chromator and Z4 may directly interact and that localization of Z4 to chromatin depends on Chromator, but not vice versa. Another candidate for mediating chromatin localization is Skeletor (Walker et al. 2000). The interaction between Chromator and Skeletor was first detected in a yeast two-hybrid screen and subsequently confirmed by pull-down assays (Rath et al. 2004). Immunocytochemical labeling of *Drosophila* embryos, S2 cells, and polytene chromosomes demonstrated that the two proteins show extensive co-localization during the cell cycle, although their distributions are not identical (Rath et al. 2004). During interphase Chromator is localized on polytene chromosomes to interband chromatin regions in a pattern that overlaps that of Skeletor. During mitosis both Chromator and Skeletor detach from the chromosomes and align together in a spindle-like structure with Chromator, additionally localizing to centrosomes that are devoid of Skeletor antibody labeling. Thus, the extensive co-localization of the two proteins is compatible with a direct physical interaction; however, at present it is not known whether such an interaction occurs throughout the cell cycle or is present only at certain stages, with additional proteins mediating complex assembly at other stages (Rath et al. 2006). Regardless, it is likely that Chromator together with Skeletor functions in at least two different molecular complexes, one associated with the spindle matrix during mitosis and one associated with nuclear and chromatin structure during interphase (Rath et al. 2004). Furthermore, taken together the findings of the present study and those of Ding et al. (2009) suggest that Chromator's chromatin functions are largely governed by the NH_2-terminal domain whereas functions related to mitosis are mediated by COOH-terminal sequences. The molecular mechanisms of how the two distinct chromatin binding affinities residing within the NH_2-terminal domain of Chromator interact to confer proper localization to interbands remains to be elucidated.

An important feature of the Chromator protein is the presence of a chromodomain, the only conserved motif found in database searches (Rath et al. 2004; Gortchakov et al. 2005). Structure determination of the prototype chromodomain has revealed a small, three-stranded antiparallel β-sheet supported by an α-helix that runs across the sheet (Ball et al. 1997; Brehm et al. 2004). Classic chromodomains contain three conserved aromatic amino acids that confer binding affinity for methylated histone H3 (Nielsen et al. 2001; Fischle et al. 2003). However, several chromodomains have been identified that vary at some of these structurally important positions but that still conform well to the overall folding of the prototype chromodomain (Brehm et al. 2004). One example of this is the chromo shadow domain also found in HP1a that is a protein–protein interaction domain that allows HP1a to homodimerize via its α-helices (Brasher et al. 2000; Cowieson et al. 2000). In addition, various chromodomains have been demonstrated to bind to a wide variety of proteins including transcription corepressors, remodeling ATPases, lamin B receptor, and chromatin assembly factors (reviewed in Jones et al. 2000). Thus, relatively small sequence variations in the otherwise conserved structural scaffold of chromodomains can confer considerable variation in molecular interactions (Brehm et al. 2004). We provide evidence by modeling that the chromodomain of Chromator is likely to adopt the canonical chromodomain tertiary configuration very similar to the chromodomain of HP1a. However, due to amino acid substitutions at two of the three conserved aromatic amino acid positions, it is not likely to bind to methylated histone H3. Rather we provide evidence by overlay and pull-down assays that it binds to the linker histone H1. A candidate region for providing such a binding fold or surface is the additional α-helical stretch found in the chromodomain of Chromator just prior to the main α-helix of the chromodomain structure. In future experiments it will be of interest to further determine the structural basis for the interaction of Chromator with histone H1 and specifically how the chromodomain contributes to Chromator's role in nucleosome and chromatin organization.

Acknowledgments We thank members of the laboratory for discussion, advice, and critical reading of the manuscript. We also wish to acknowledge Mr. Atres Norwood for technical assistance. This work was supported by NSF Grant MCB0817107 and NIH grant GM062916 (KMJ/JJ).

References

Ball LJ, Murzina NV, Broadhurst RW, Raine AR, Archer SJ, Stott FJ, Murzin AG, Singh PB, Domaille PJ, Laue ED (1997) Structure of the chromatin binding (chromo) domain from mouse modifier protein 1. EMBO J 16:2473–2481

Brand AH, Perrimon N (1993) Targeted gene expression as a means of altering cell fates and generating dominant phenotypes. Development 118:401–415

Brasher SV, Smith BO, Fogh RH, Nietlispach D, Thiru A, Nielsen PR, Broadhurst RW, Ball LJ, Murzina NV, Laue ED (2000) The structure of mouse HP1 suggests a unique mode of single peptide recognition by the shadow chromo domain dimer. EMBO J 19:1587–1597

Brehm A, Tufteland KR, Aasland R, Becker PB (2004) The many colours of chromodomains. Bioessays 26:133–140

Cai W, Jin Y, Girton J, Johansen J, Johansen KM (2010) Preparation of polytene chromosome squashes for antibody labeling. *J. Vis. Exp.* http://www.jove.com/index/Details.stp?ID=1748

Cowieson NP, Partridge JF, Allshire RC, McLaughlin PJ (2000) Dimerization of a chromo shadow domain and distinctions from the chromodomain as revealed by structural analysis. Curr Biol 10:517–525

Deng H, Zhang W, Bao X, Martin JN, Girton J, Johansen J, Johansen KM (2005) The JIL-1 kinase regulates the structure of *Drosophila* polytene chromosomes. Chromosoma 114:173–182

Ding Y, Yao C, Lince-Faria M, Rath U, Cai W, Maiato H, Girton J, Johansen KM, Johansen J (2009) Chromator is required for proper microtubule spindle formation and mitosis in *Drosophila*. Dev Biol 334:253–263

Eggert H, Gortchakov A, Saumweber H (2004) Identification of the *Drosophila* interband-specific protein Z4 as a DNA-binding zinc-finger protein determining chromosomal structure. J Cell Sci 117:4253–4264

Fischle W, Wang Y, Jacobs SA, Kim Y, Allis CD (2003) Molecular basis for the discrimination of repressive methyl-lysine marks in histone H3 by Polycomb and HP1 chromodomains. Genes Dev 17:1870–1881

Gan M, Moebus S, Eggert H, Saumweber H (2011) The Chriz-Z4 complex recruits JIL-1 to polytene chromosomes, a requirement for inter-band-specific phosphorylation of H3S10. J Biosci 36:425–438

Gortchakov AA, Eggert H, Gan M, Mattow J, Zhimulev IF, Saumweber H (2005) Chriz, a chromodomain protein specific for the interbands of *Drosophila melanogaster* polytene chromosomes. Chromosoma 114:54–66

Hill RJ, Watt F, Wilson CM, Fifis T, Underwood PA, Tribbick G, Geysen HM, Thomas JO (1989) Bands, interbands and puffs in native *Drosophila* polytene chromosomes are recognized by a monoclonal antibody to an epitope in the carboxy-terminal tail of histone H1. Chromosoma 98:411–421

Jacobs SA, Khorasanizadeh S (2002) Structure of HP1 chromodomain bound to a Lysine 9-methylated histone H3 tail. Science 295:2080–2083

Jin Y, Wang Y, Walker DL, Dong H, Conley C, Johansen J, Johansen KM (1999) JIL-1: a novel chromosomal tandem kinase implicated in transcriptional regulation in *Drosophila*. Mol Cell 4:129–135

Johansen KM, Forer A, Yao C, Girton J, Johansen J (2011) Do nuclear envelope and intranuclear proteins reorganize during mitosis to form an elastic, hydrogel-like spindle matrix? Chromosome Res 19:345–365

Jones DO, Cowell IG, Singh PB (2000) Mammalian chromodomain proteins: their role in genome organization and expression. Bioessays 22:124–137

Khorasanizadeh S (2004) The nucleosome: from genomic organization to genomic regulation. Cell 116:259–272

Kusch T, Guelman S, Abmayr SM, Workman JL (2003) Two *Drosophila* Ada2 homologues function in different multiprotein complexes. Mol Cell Biol 23:3305–3319

Lindsley DL, Zimm GG (1992) The genome of *Drosophila melanogaster*. Academic, New York

Mendjan S, Taipale M, Kind J, Holz H, Gebhardt P, Schelder M, Vermeulen M, Buscaino A, Duncan K, Mueller J, Wilm M, Stunnenberg HG, Saumweber H, Akhtar A (2006) Nuclear pore components are involved in the transcriptional regulation of dosage compensation in *Drosophila*. Mol Cell 21:811–823

Nielsen AL, Oulad-Abdelghani M, Ortiz JA, Remboutsika E, Chambon P, Losson R (2001) Heterochromatin formation in mammalian cells: interaction between histones and HP1 proteins. Mol Cell 7:729–739

Nowak SJ, Pai C-Y, Corces VG (2003) Protein phosphatase 2A activity affects histone H3 phosphorylation and transcription in *Drosophila melanogaster*. Mol Cell Biol 23:6129–6138

Paro R, Hogness D (1991) The Polycomb protein shares a homologous domain with a heterochromatin associated protein of *Drosophila*. Proc Natl Acad Sci USA 88:263–267

Qi H, Rath U, Wang D, Xu Y-Z, Ding Y, Zhang W, Blacketer M, Paddy M, Girton J, Johansen J, Johansen KM (2004) Megator, an essential coiled-coil protein localizes to the putative spindle matrix during mitosis. Mol Biol Cell 15:4854–4865

Qi H, Rath U, Ding Y, Ji Y, Blacketer MJ, Girton J, Johansen J, Johansen KM (2005) EAST interacts with Megator and localizes to the putative spindle matrix during mitosis in *Drosophila*. J Cell Biochem 95:1284–1291

Rath U, Wang D, Ding Y, Xu Y-Z, Qi H, Blacketer MJ, Girton J, Johansen J, Johansen KM (2004) Chromator, a novel and essential chromodomain protein interacts directly with the putative spindle matrix protein Skeletor. J Cell Biochem 93:1033–1047

Rath U, Ding Y, Deng H, Qi H, Bao X, Zhang W, Girton J, Johansen J, Johansen KM (2006) The chromodomain protein, Chromator, interacts with JIL-1 kinase and regulates the structure of *Drosophila* polytene chromosomes. J Cell Sci 119:2332–2341

Roberts DB (1998) In *Drosophila*: a practical approach. (Oxford: IRL), pp 295

Roy A, Kucukural A, Zhang Y (2010) I-TASSER: a unified platform for automated protein structure and function prediction. Nat Protoc 5:725–738

Sambrook J, Russell DW (2001) Molecular cloning: a laboratory manual. Cold Spring Harbor Laboratory, New York

Siriaco G, Deuring R, Chioda M, Becker PB, Tamkun JW (2009) Drosophila ISWI regulates the association of histone H1 with interphase chromosomes in vivo. Genetics 182:661–669

Towbin H, Staehelin T, Gordon J (1979) Electrophoretic transfer of proteins from polyacrylamide gels to nitrocellulose sheets: procedure and some applications. Proc Natl Acad Sci USA 76:4350–4354

Walker DL, Wang D, Jin Y, Rath U, Wang Y, Johansen J, Johansen KM (2000) Skeletor, a novel chromosomal protein that redistributes during mitosis provides evidence for the formation of a spindle matrix. J Cell Biol 151:1401–1411

Wang Y, Zhang W, Jin Y, Johansen J, Johansen KM (2001) The JIL-1 tandem kinase mediates histone H3 phosphorylation and is required for maintenance of chromatin structure in *Drosophila*. Cell 105:433–443

Wasser M, Osman ZB, Chia W (2007) EAST and Chromator control the destruction and remodeling of muscles during *Drosophila* metamorphosis. Dev Biol 307:380–393

Zhang Y (2007) Template-based modeling and free modeling by I-TASSER in CASP7. Proteins 68:108–117

Zhang Y (2008) Progress and challenges in protein structure prediction. Curr Opin Struct Biol 18:342–348